Sensors and Actuators B 174 (2012) 279–284

Contents lists available at SciVerse ScienceDirect

Sensors and Actuators B: Chemical

journal homepage: www.elsevier.com/locate/snb

How low does the oxygen concentration go within a sandwich-type amperometric biosensor?

Marcelo Ricardo Romero, Ana M. Baruzzi, Fernando Garay*

INFIQC, Dpto. de Físico Química, Facultad de Ciencias Químicas, UNC, Pab. Argentina, ala 1, 2° piso, Ciudad Universitaria, 5000 Córdoba, Argentina

ARTICLE INFO

Article history:
Received 18 June 2012
Received in revised form 8 August 2012
Accepted 14 August 2012
Available online xxx

Keywords:
Ping-pong
Simplex
Amperometric sensor
Sandwich-type biosensor
Hydrogel
Oxidase

ABSTRACT

Software for the automatic non-linear least squares fit of chronoamperometric responses corresponding to sandwich-type amperometric biosensors has been developed. The so-called Simplex algorithm computes a minimum value for the difference between experimental and theoretical data. The latter consider a numerical model based on a ping-pong reaction mechanism corresponding to an oxidase enzyme that has been immobilized between diffusion membranes.

The results obtained from the simulation of a first-generation lactate biosensor in presence of 0.1 mM substrate indicate that the concentration of O_2 would decrease only 0.1% with regards to its bulk value. Besides, the concentration of this natural mediator would remain practically unchanged during a typical calibration curve. This is because the rather high diffusion coefficient of O_2 and its regeneration at the electrode surface minimize the concentration changes of this species. In addition, it was found that the thicknesses of polycarbonate membranes and the enzymatic matrix have average values of 13 μm and 20 μm, respectively. However, these membranes might exhibit smaller thickness depending on the time provided for the crosslinking reaction. In this regard, if this reaction is slow enough, the enzymatic matrix would be able to diffuse through the pores of polycarbonate membranes and they will appear to be thinner than expected. This effect may compromise the response-time and the reproducibility of this kind of biosensors.

© 2012 Elsevier B.V. All rights reserved.

1. Introduction

The high specificity of enzymes enabled the development of biosensors, which are devices that can recognize specific substrates in samples with very complex matrixes [1–6]. The enzymatic reaction is typically detected by electrochemical or spectroscopical transducers [4–12]. A widely used detection strategy corresponds to the amperometric biosensors that use an oxidoreductase enzyme for changing the oxidation state of the substrate [1–6]. The reaction of several oxidases such as glucose oxidase or lactate oxidase can be represented by the following ping-pong mechanism [1,2,13]:

$$E_r + S \underset{k_{-1}}{\overset{k_1}{\rightleftarrows}} E_rS \overset{k_2}{\rightarrow} E_o + R \quad (1)$$

$$E_o + M \underset{k_{-3}}{\overset{k_3}{\rightleftarrows}} E_oM \overset{k_4}{\rightarrow} E_r + P \quad (2)$$

where E_r and E_o are the reduced and oxidized forms of the enzyme, M is the mediator, while R and P are products of the enzymatic reaction. The species E_rS and E_oM are intermediate complexes of the enzyme with S and M, respectively. From the analysis of Eqs. (1) and (2) it is possible to obtain the expression that describes the velocity of an enzymatic reaction according to a ping-pong scheme [13–18]:

$$v = \frac{v_{max}}{1 + K_S/C_S + K_M/C_M} \quad (3)$$

In this expression $v_{max} = C_E k_2 k_4 \ [(k_2 + k_4)]^{-1} = C_E k_{cat}$, $K_S = k_4 (k_{-1} + k_2) \ [(k_2 + k_4)k_1]^{-1}$, and $K_M = k_2 \ (k_{-3} + k_4) \ [(k_2 + k_4)k_3]^{-1}$. The constants K_S and K_M are usually called Michaelis' constants for S and M, C_E is the total concentration of the enzyme, and the variables C_M and C_S indicate the concentrations for M and S, respectively.

The electrochemical step for most amperometric biosensors can be represented by the following reaction:

$$P \overset{-ne^-}{\rightarrow} M \quad (4)$$

where the enzymatic product P is electrochemically oxidized to regenerate M. If the species P and M correspond to H_2O_2 and O_2, the device is denominated a first-generation biosensor [5,16]. However, if this natural redox mediator is replaced by another artificial electron carrier such as metallic complexes, then it is named

* Corresponding author. Tel.: +54 351 4334169/80; fax: +54 351 4334188.
E-mail addresses: fgaray@fcq.unc.edu.ar, fsgaray@gmail.com (F. Garay).

0925-4005/$ – see front matter © 2012 Elsevier B.V. All rights reserved.
http://dx.doi.org/10.1016/j.snb.2012.08.027

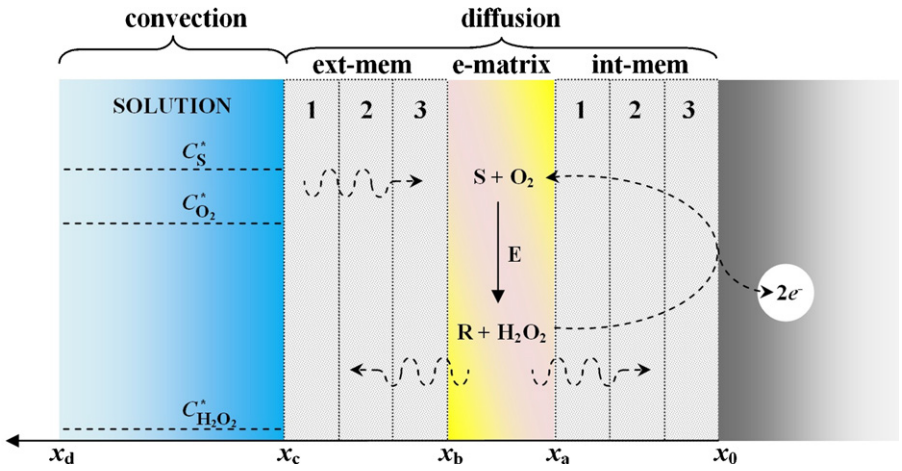

Fig. 1. Scheme of a sandwich-type amperometric biosensor. The numbers indicate different diffusion membranes.

second-generation biosensor [5,17]. Although oxygen is cheaper and more stable than any other artificial mediator, the oxidation of H_2O_2 requires a rather high potential at which other interfering species can react [5,13,17,19]. In addition, the concentration of oxygen is low and it is believed that it might compromise the stoichiometry of the enzymatic reaction [17–20]. Since most interfering species are negatively charged at pH 7, the first drawback can be minimized by coating the electrode surface with Nafion [5,21]. The second problem could be solved by using a membrane that tailors the diffusion of oxygen with regards to other reagents [5,13]. Both strategies have been implemented for optimizing sandwich-type amperometric biosensors, which are typically devices of first-generation [5,13]. Nevertheless, it is difficult or even impossible to measure the concentration profile of O_2 into the E-matrix, without disturbing the normal function of the sensor. Actually, it is also hard to assess several other variables of the sensor and for this reason, most advances on the area are based on a number of hypothesis that intend to explain why a calibration curve provides better or worse result than others.

The aim of this work is to apply a recently developed model to fit experimental chronoamperometric transients [13]. This procedure would let us estimate the concentration profiles of involved species within a sandwich-type amperometric biosensor as well as other parameters such as the thickness of the membrane and the E-matrix.

2. The model

The boundary conditions of this model are related to a sandwich-type amperometric biosensor, where the enzyme is confined within the E-matrix such as the scheme of Fig. 1. It is considered that, before the addition of the substrate, the concentrations of E and M are constants and the values of C_S and C_P are equal to zero. The species P can be rapidly re-oxidized at the electrode surface, and the effects associated with the migration of species can be neglected [22,23]. More details about the model can be consulted in a previous manuscript [13].

The equations used for the evaluation of concentration profiles are the following [13].

For $(x_c \geq x > x_b)$ and $(x_a \geq x > x_0)$:

$$(C_i)_j^{t+1} = (C_i)_j^t + \frac{D_i \delta t}{\delta x^2}\left[(C_i)_{j-1}^t - 2(C_i)_j^t + (C_i)_{j+1}^t\right] \quad (5)$$

For $(x_b \geq x > x_a)$:

$$(C_i)_j^{t+1} = (C_i)_j^t + \frac{D_i \delta t}{\delta x^2}\left[(C_i)_{j-1}^t - 2(C_i)_j^t + (C_i)_{j+1}^t\right] \pm \frac{v_{max}}{1 + K_S/(C_i)_j^t + K_M/(C_i)_j^t} \quad (6)$$

The thickness of most real sandwich-type biosensors (Δx) goes between 10 and 100 μm, where the x-axis is normal to the electrode surface and δx corresponds to the grid-size [19,22,24]. The subindex i represents some of the involved species, while j corresponds to a given position within the membrane [13]. The sign minus is used to evaluate the concentration profiles of S and M while the sign plus is employed for the case of species P and R. At the electrode surface ($x = 0$):

$$\Psi(\tau) = \frac{I(\tau)}{n_e FAC_S^*}\frac{\tau}{\delta x} = \frac{D_P \delta t N}{\delta x^2}\frac{(C_P)_1^t}{C_S^*} \quad (7)$$

In the last expression, $\Psi(\tau)$ corresponds to the dimensionless current at the time $\tau = N\Delta t$. The dimensionless diffusion of the mediator was fixed as: $D_M \delta t/\delta x^2 = 0.40$ [13]. Eq. (7) provides the theoretical transients that need to be fitted to experimental profiles.

The fit of experimental data with theoretical curves requires an algorithm that automatically minimizes the difference between every calculated and measured data point [25–29]. The Simplex algorithm calculates the goodness of fit (f^2) by the following expression of minimum-squares [27]:

$$f^2 = \sum_{t=1}^{\Omega}\left[\frac{I_{exp,t} - I_{cal,t}}{I_{exp,\Omega}}\right]^2 \Omega^{-1}$$

where $I_{exp,\Omega}$ is the experimental limiting-current, $I_{exp,t}$ and $I_{cal,t}$ are the experimental and calculated values of current, and Ω indicates the number of experimental data points. This fitting algorithm requires a set of starting values (seeds) that the researcher has to estimate in order to calculate the first theoretical curve [25–28]. Then the Simplex algorithm automatically changes these values to optimize the fit of the experimental profile, which is in fact a minimum of f^2 [28]. It is critical to provide a good set of seeds, otherwise either the simulated curve will not match the experiment or the out coming results will be meaningless [26,27]. Concerning this last point, it is suggested to compare the results of a set of experimental profiles instead of fitting isolated curves [25–27]. Such comparison helps the researcher to realize about the values of

some variables and/or to find out some misleading results during the fit.

3. Materials and methods

3.1. Reagents

All solutions were prepared with ultra pure water (18 MΩ cm^{-1}) from a Millipore Milli-Q system. The base electrolyte solution (0.1 M) consisted in 0.05 M HK_2PO_4/0.05 M H_2KPO_4 (Merck, Germany). This solution was renewed weekly and small amounts of H_2SO_4 (Baker, USA) or KOH (Merck, Germany) were used to fix it at pH 7.0. Stock solutions of 0.1 M lactate (Sigma, USA) and 5% (v/v) glutaraldehyde (Backer, USA) were prepared in the base electrolyte. A total amount of 100 U LOD from Pediococus species (Sigma, USA) was dissolved in 1000 μL of base electrolyte. Then, the solution was separated into aliquots of 20 μL and stored at −20 °C. Thus, every aliquot bears 2 U of LOD. Mucin (Sigma, USA) was mortared and stored as dry powder at 4 °C. Bovine serum albumin (Sigma, USA) was used as received. All solutions were stored at 4 °C. All reagents were of analytical grade and used as received. Polycarbonate membranes of 0.05 μm pore size were cut in discs of 6 mm diameter (Millipore, USA).

3.2. Apparatus

All electrochemical experiments were performed with an Autolab PGSTAT 30 Electrochemical Analyzer (Eco Chemie, The Netherlands). The measurements were carried out using a conventional three-electrode system. The working electrode was a 2 mm diameter Pt disc (CH Instruments, USA), while a Pt wire was the counter electrode, and a Ag|AgCl|KCl(3 M) (CH Instruments, USA) was the reference electrode. Amperometric detection was carried out under batch conditions and the solution was stirred at 120 rpm during the whole electrochemical experiment.

3.3. Construction of the enzymatic electrode

In this work the strategy for preparing the enzymatic LOD-matrix is the same than that described previously [30]. Shortly, 6.0 mg of a mixture 70/30 mucin/albumin was dissolved in 40 μL of base electrolyte and then transferred into a vial containing 2 U of LOD. Each enzymatic electrode was prepared using an aliquot of 6 μL LOD-matrix mixed with 3 μL of glutaraldehyde. The resulting hydrogel was entrapped between two membranes of polycarbonate. After waiting 5 min, buffer solution was used to rinse the electrode and eliminate glutaraldehyde molecules that did not react in the E-matrix.

3.4. Calculations

All calculations were performed in Fortran 90 with an Intel Visual Fortran Compiler for Microsoft Visual Studio 2008. The time required for each simulated curve was around 5 s when a laptop with an Intel Core i3 processor of 330 MHz was used. Once the proper set of seeds has been found, the Simplex algorithm usually requires less than 50 iterations to achieve a minimum value of f^2.

4. Results and discussion

4.1. Numerical errors vs. experimental limitations

Every fitting protocol has an error related to the assumptions of the model and, in the case of numerical solutions, to the grid-size (δx) [31]. The assumptions that characterize the model are described above and more details of this mathematical approach can be found in a previous manuscript [13]. Fig. 2 shows the errors introduced to the dimensionless steady-state current (Ψ_{ss}) and to the concentration of involved species when grids of different size are used. This analysis is performed evaluating the dependence of the relative error on the concentration of substrate. The concentrations of species are calculated using the average value of each reagent into the E-matrix and once the steady-state condition has been achieved. The numerical error is evaluated from the difference of curves determined with grids of diverse size and "overconverged" results [31]. The latter corresponds to the use of a grid of 0.1 μm, which ensures very good precision for the calculations, but requires around an hour to get every simulated profile. However, such a high precision would not be necessary since the experimental sensor-to-sensor reproducibility typically goes between 1 and 5% [19,30]. Moreover, Millipore informs that the thickness of its polycarbonate membranes is between 7 and 22 μm, indicating that these films may be not entirely flat in the micrometric scale either [32]. The roughness of other membranes should be even more significant, since they would not have the smooth glass-like surface of polycarbonate membranes. Accordingly, it would not be necessary to use a grid of very small size. Instead of it, a grid with numerical error around 1% that provides fast results is preferred.

All calculations shown in Fig. 2 were done considering a biosensor with $\Delta x = 100$ μm, where the E-matrix has a thickness of 34 μm and the diffusion membranes are both of 33 μm. Fig. 2A shows that the numerical error is around 0.5% for a grid of 1 μm, curve (b), while the error is higher than 1% for grids larger than 2 μm, curves (c–e). The error of Ψ_{ss} is more important when the value of C_S is close to 6 mM. Similar behavior is observed for C_P in the enzymatic matrix ($C_{P,EM}$), Fig. 2B. For the higher value of C_S, the lower relative error is computed for this parameter into the enzymatic matrix ($C_{S,EM}$). Conversely, the value calculated for C_M presents higher relative error when C_S is increased, Fig. 2D. This is because more amount of mediator is consumed when the enzyme is in presence of a high concentration of substrate. As a result of this analysis, and taking in mind that the thickness of its polycarbonate membranes may vary from 8 to 20 μm, it was selected the grid of 1 μm for fitting the different experimental profiles [32].

4.2. Fitting chronoamperometric transients

Fig. 3 shows experimental (circles) and simulated (lines) chronoamperometric profiles corresponding to a lactate biosensor prepared with different number of external membranes. As indicated in the experimental section, the external polycarbonate membrane was placed on top of the E-matrix right after the addition of glutaraldehyde. Five minutes later, buffer was added to stop the reaction [30]. Once the first sandwich was prepared, the subsequent membranes were added to the sensor. In consequence, it is obtained a set of profiles with similar values of limiting current, but different response-time [13]. For the analysis of these transients, it was considered that $C_M = 0.274$ mM, which is the saturated oxygen concentration in blood [33]. The values of K_M, K_S, and k_{cat} are well-known [14], while D_P and D_M into the sandwich biosensor were assumed to be the half of their values in aqueous solution [34]. With regards to the concentration of the active enzyme within the E-matrix, it was estimated a value of $C_E = 1$ μM by using a formula weight of 350 kDa [35]. As an additional constraint it was required that the Simplex algorithm had to provide the same values for the thicknesses of the E-matrix and of the inner membrane. After several fits it was found that all profiles could be fitted with a rather low value of f^2 when the thicknesses of the E-matrix and of the inner membrane were 20 μm and 4 μm, respectively. Accordingly, those values were set as constants and the software had to

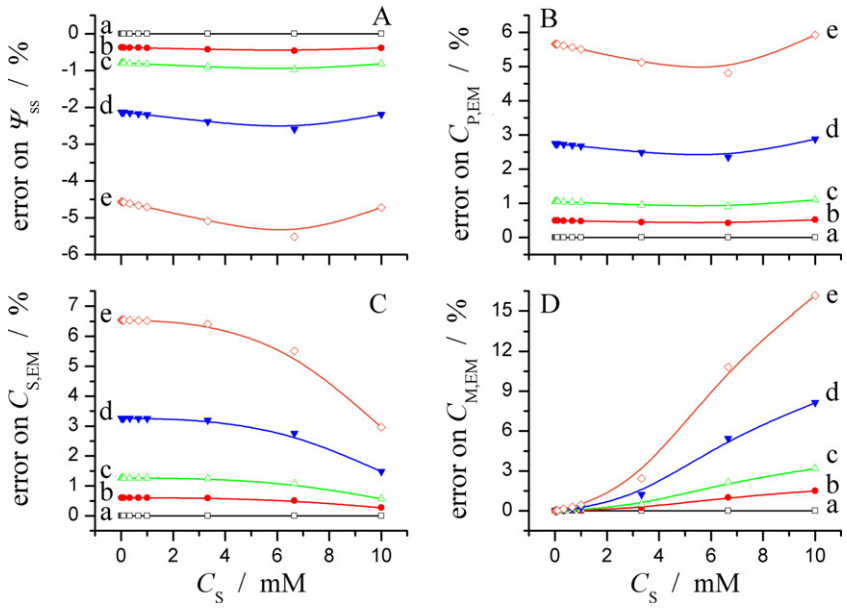

Fig. 2. Dependence of the relative error of: (A) Ψ_{ss}, (B) C_P, (C) C_S, and (D) C_M on the grid size used. The concentration of every species has been averaged into the E-matrix under steady-state conditions. $C_M = 0.274$ mM, $D_S = 1 \times 10^{-6}$ cm^2 s^{-1}, $D_P = 5 \times 10^{-6}$ cm^2 s^{-1}, $D_M = 1 \times 10^{-5}$ cm^2 s^{-1}, $K_M = 7.1 \times 10^{-5}$ M, $K_S = 2.2 \times 10^{-2}$ M, $\Delta x = 100$ μm, $\tau = 200$ s, $v_{max} = 0.10$ mM s^{-1}, and grid size/μm = (a) 0.1, (b) 1, (c) 2, (d) 5, and (e) 10.

minimize only three variables: the thickness of the sandwich (Δx), D_{Lac}, and a scaling factor. From this second set of fits, it was found that the scaling factor = 0.05, while D_{Lac} decreased from 5×10^{-6} cm^2 s^{-1} to 3×10^{-6} cm^2 s^{-1} according to the number of membranes was increased. With regards to Δx the fits pointed out that this variable depends linearly on the number of external membranes, see Fig. 3B. Moreover, from the linear regression of these data it was determined a slope of (14 ± 1) μm, which would be the thickness of every polycarbonate membrane added to the sensor. This result is in agreement with Millipore's specifications since they inform that the thickness of these membranes ranges from 7 to 22 μm [32]. The most relevant data obtained from these fits can be consulted in Supporting information, Table S1.

Curiously, the membranes that are directly bounded to the E-matrix evidenced smaller thickness than the others. The values calculated for the inner and outer membranes are 4 and 5 μm, respectively. In order to study this outcome, a new sandwich-type biosensor was prepared. In this case, after the addition of glutaraldehyde, we wait for 5 min before placing the external polycarbonate membrane. In consequence, the E-matrix was already a hydrogel at the time that the external membrane was placed. Fig. 4 shows experimental (circles) and simulated (lines) chronoamperometric profiles corresponding to this second lactate biosensor. After recording the first chronoamperogram, an additional polycarbonate membrane was placed between the sandwich and the electrode surface. The same procedure was performed for the subsequent membranes.

The fits were carried out using the same parameters than before. After the required preliminary set of fits it was found that thicknesses of the E-matrix and the external membrane could be estimated as 20 μm and 13 μm, respectively. With regards to

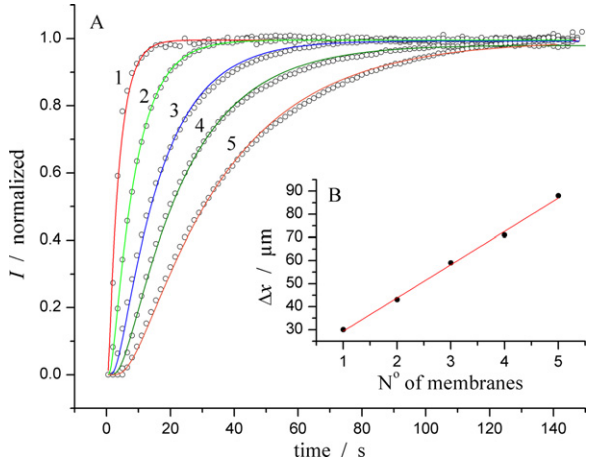

Fig. 3. (A) Experimental (circles) and simulated (lines) normalized current transients measured for different number of external membranes and (B) dependence of the calculated external membrane thickness on the number of membranes. The parameters used for the fits are: $C_M = 0.274$ mM, $D_P = 5 \times 10^{-6}$ cm^2 s^{-1}, $D_M = 1 \times 10^{-5}$ cm^2 s^{-1}, $K_M = 7.1 \times 10^{-5}$ M, $K_S = 2.2 \times 10^{-2}$ M, $v_{max} = 0.10$ mM s^{-1}, $C_S = 0.1$ mM, thicknesses of inner membrane = 4 μm, and thickness of the E-matrix = 20 μm.

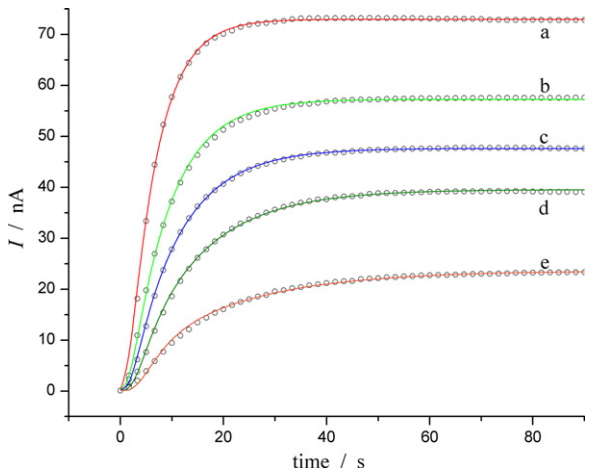

Fig. 4. Experimental (circles) and simulated (lines) current transients measured for different number of inner membranes. The parameters used for the fits are: $C_M = 0.274$ mM, $D_P = 5 \times 10^{-6}$ cm^2 s^{-1}, $D_M = 1 \times 10^{-5}$ cm^2 s^{-1}, $K_M = 7.1 \times 10^{-5}$ M, $K_S = 2.2 \times 10^{-2}$ M, $v_{max} = 0.10$ mM s^{-1}, $C_S = 0.1$ mM, thicknesses of outer membrane = 13 μm, and thickness of the E-matrix = 20 μm.

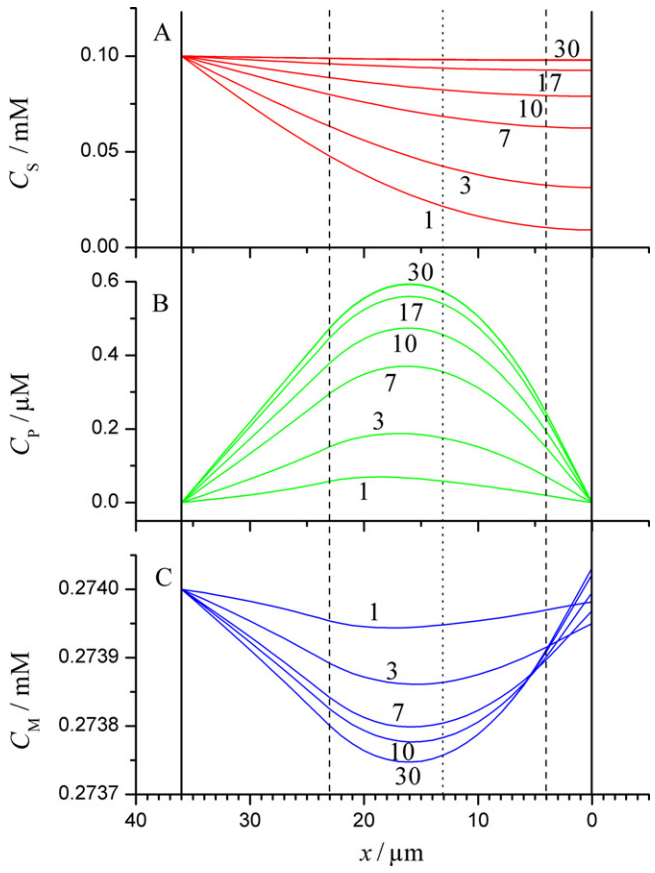

Fig. 5. Dependence of (A) C_S, (B) C_P, and (C) C_M on the distance from the electrode surface of a sandwich-type biosensor. The numbers indicate the seconds elapsed after the addition of the substrate. Full straight lines are the edges of the sensor. Dashed lines are the limits of the E-matrix. Parameters employed: $C_M = 0.274$ mM, $D_S = 5.5 \times 10^{-6}$ cm^2 s^{-1}, $D_P = 5 \times 10^{-6}$ cm^2 s^{-1}, $D_M = 1 \times 10^{-5}$ cm^2 s^{-1}, $K_M = 7.1 \times 10^{-5}$ M, $K_S = 2.2 \times 10^{-2}$ M, $v_{max} = 0.10$ mM s^{-1}, $C_S = 0.1$ mM, $\Delta x = 36$ μm, thicknesses of outer membrane = 13 μm, and thickness of the E-matrix = 20 μm.

this last value, we should remember that the external membrane was placed when the E-matrix was already a hydrogel. In a similar way than before, these values were used as constraints for the subsequent fits. Thus, it was also necessary to fit three variables: Δx, D_{Lac}, and the scaling factor. Again an average value of $(4 \pm 1) \times 10^{-6}$ cm^2 s^{-1} is found for D_{Lac}. The thickness of the sensor also increased linearly with the number of inner membranes and the value obtained for the scaling factor was equal to 0.3 nA. The numerical data resulting from these fits can be found in Supporting information, Table S2.

The parameters obtained from the fit of curve (a) in Fig. 4 were used to calculate the concentration profiles of involved species in the sandwich-type amperometric biosensor. These data are shown in Fig. 5. The concentration profiles of lactate (C_S), H_2O_2 (C_P) and O_2 (C_M) are analyzed as functions of the distance from the electrode surface in Fig. 5(A)–(C), respectively. These figures also show the evolution of those profiles on time. In this regard, the numbers correspond to the seconds elapsed after the addition of the substrate. The full straight lines of the figure intend to show the boundaries of the sensor, while the dashed lines would point out the limits of the E-matrix. As it can be observed, C_S diminishes at the beginning of the experiment, but it practically reestablishes the concentration of the bulk after 30 s. At any time the transient of current depends on the value of C_P within the sensor, which is determined by the enzyme kinetics and by its own diffusion through the membranes, Eqs. (1)–(6). As a consequence of this, simple analytical equations can be used for calculating the limiting current, but not for analyzing the whole chronoamperometric response of this kind of sensors.

After 30 s the concentration of H_2O_2 reaches its maximum value in the E-matrix, Fig. 5B. Under these conditions the value of C_P is around 0.5 μM into the E-matrix and this value would linearly increase within the linear range of the sensor. Even though the concentration of O_2 exhibits a minimum in the E-matrix, this diminution corresponds only to 0.1% of its concentration in the bulk. When the same calculation was performed for a solution with $C_S = 1$ mM, the value of C_M would have diminished to 0.271 mM from 0.274 mM. The reason for this insignificant change on the concentration of O_2 is related to the regeneration of this species at the electrode surface, and to the fast diffusion with regards to the other reagents. Besides, sandwich-type biosensors are rarely exposed to higher concentrations of substrate, since blood samples are diluted [13,36].

As indicated above, the thicknesses estimated for the outer and inner membranes are 13 and 4 μm, respectively. Conversely, if the external membrane is placed right after the addition of glutaraldehyde, the thicknesses calculated for the membranes that are directly bounded to the E-matrix were both around 4 μm, Fig. 2. To explain this, it is necessary to consider the preparation of the biosensor. In this regard, the E-matrix consists on a solution of macromolecules that can diffuse through the holes of polycarbonate membranes. Once the glutaraldehyde has been added, the E-matrix becomes a hydrogel that cannot escape from the sandwich. Consequently, polycarbonate membranes appear to be thinner than expected because they have been partially filled with the E-matrix. Thus, when the external membrane is placed after the crosslinking reaction, the E-matrix can only diffuse through the inner membrane. This effect has been schematized in Fig. 5 where dashed lines indicate the thickness of the E-matrix while the dotted line would point out the actual limit of the inner membrane. The diffusion of the E-matrix into the membranes does not only affect the thickness, but also the response-time of a sandwich-type biosensor. For this reason the response indicated by curve (a) in Fig. 3 requires 11 s to reach 95% of the limiting current while the one of Fig. 4 needs 18 s. In brief, the thickness of the external membrane affects the response time, while the one of the inner membrane controls the sensitivity of the biosensor, see Figs. 3 and 4.

5. Conclusions

The fit of experimental results of a sandwich-type amperometric biosensor has been performed using a numerical model coupled to the Simplex algorithm. The software was used to fit chronoamperometric profiles corresponding to a lactate biosensor in which the number of inner and outer membranes was varied. These well controlled conditions were used to validate the model and to explain some characteristics of sandwich-type biosensors.

From the analysis of these curves it was found that the concentration of O_2 would be practically unchanged after the addition of 0.1 mM of substrate. Moreover, the addition of 1 mM substrate would only decrease C_M in 1%, for a stirred system that is typically saturated with oxygen. The high diffusion coefficient of O_2 with regards to the one of the substrate and its regeneration at the electrode surface minimize the concentration changes of this mediator. Those minor changes calculated for the concentration of O_2 should not affect at all the linear response of first-generation biosensors with sandwich-type configuration.

The thickness of polycarbonate membranes would have an average value of 13 μm, which is well in the range informed by Millipore. Besides, the thickness of the E-matrix was estimated in 20 μm and this value would not significantly change provided the same experimental conditions are used. In this regard, it is

imperative to control the time in which the crosslinker agent is added, since it would determine the degree in which the E-matrix diffuses through the membranes.

With the data obtained in this work it is possible to go further and evaluate the effect of other variables such as the concentration of enzyme, the concentration of crosslinker, and the matrix composition. These variables will be discussed in a future manuscript since it is necessary to consider more parameters such as the aqueous/matrix distribution coefficient. The Simplex algorithm automatically minimizes the difference between the experiment and a theoretical curve. However, the researcher has to decide what result has more physical meaning from a set of local minima.

Acknowledgments

This work was funded by FONCYT, CONICET, and Secyt-UNC. F. Garay and A. Baruzzi are research fellows of CONICET.

Appendix A. Supplementary data

Supplementary data associated with this article can be found, in the online version, at http://dx.doi.org/10.1016/j.snb.2012.08.027.

References

[1] A. Heller, B. Feldman, Electrochemical glucose sensors and their applications in diabetes management, Chemical Reviews 108 (2008) 2482–2505.
[2] P.-C. Nien, P.-Y. Chen, K.-C. Ho, in: V.S. Somerset (Ed.), Intelligent and Biosensors, Vukovar, Croatia, 2010, pp. 245–268.
[3] A. Sassolas, L.J. Blum, B.D. Leca-Bouvier, Immobilization strategies to develop enzymatic biosensors, Biotechnology Advances 30 (2012) 489–511.
[4] C. Dhand, M. Das, M. Datta, B.D. Malhotra, Recent advances in polyaniline based biosensors, Biosensors and Bioelectronics 26 (2011) 2811–2821.
[5] J. Wang, Electrochemical glucose biosensors, Chemical Reviews 108 (2008) 814–825.
[6] L. Campanella, A. Nuccilli, M. Tomassetti, S. Vecchio, Biosensor analysis for the kinetic study of polyphenols deterioration during the forced thermal oxidation of extra-virgin olive oil, Talanta 74 (2008) 1287–1298.
[7] I. Barman, C.-R. Kong, G.P. Singh, R.R. Dasari, M.S. Feld, Accurate spectroscopic calibration for noninvasive glucose monitoring by modeling the physiological glucose dynamics, Analytical Chemistry 82 (2010) 6104–6114.
[8] B.D. Malhotra, A. Chaubey, Biosensors for clinical diagnostics industry, Sensors and Actuators B 91 (2003) 117–127.
[9] F.S. Ligler, Perspective on optical biosensors and integrated sensor systems, Analytical Chemistry 81 (2009) 519–526.
[10] A. Mulchandani, K.R. Rogers, Enzymes and Microbial Biosensors: Techniques and Protocols, Humana Press Inc., NJ, USA, 1998.
[11] Q. Wu, L. Wang, H. Yu, J. Wang, Z. Chen, Organization of glucose-responsive systems and their properties, Chemical Reviews 111 (2011) 7855–7875.
[12] P.T. Kissinger, Biosensors – a perspective, Biosensors and Bioelectronics 20 (2005) 2512–2516.
[13] M.R. Romero, A.M. Baruzzi, F. Garay, Mathematical modeling and experimental results of a sandwich-type amperometric biosensor, Sensors and Actuators B 162 (2012) 284–291.
[14] S. Ghisla, V. Massey, in: F. Müller (Ed.), Lactate Oxidase, Chemistry and Biochemistry of Flavoenzymes, vol. 2, CRC Press, FL, USA, 1991, pp. 243–289.
[15] R. Krishnan, P. Atanasov, E. Wilkins, Mathematical modeling of an amperometric enzyme electrode based on a porous matrix of Stöber glass beads, Biosensors and Bioelectronics 11 (1996) 811–822.
[16] J.W. Parker, C.S. Schwartz, Modeling the kinetics of immobilized glucose oxidase, Biotechnology and Bioengineering 30 (1987) 724–735.
[17] D.A. Gough, J.Y. Lucisano, P.H.S. Tse, Two-dimensional enzyme electrode sensor for glucose, Analytical Chemistry 57 (1985) 2351–2357.
[18] R. Baronas, J. Kulys, Modelling amperometric biosensors based on chemically modified electrodes, Sensors 8 (2008) 4800–4820.
[19] I. Iliev, P. Atanasov, S. Gamburzev, A. Kaisheva, V. Tonchev, Transient response of electrochemical biosensors with asymmetrical sandwich membranes, Sensors and Actuators B 8 (1992) 65–72.
[20] A.E.G. Cass, G. Davis, G.D. Francis, H.A. Hill, W.J. Aston, I.J. Higgins, E.V. Plotkin, L.D.L. Scott, A.P.F. Turner, Ferrocene-mediated enzyme electrode for amperometric determination of glucose, Analytical Chemistry 56 (1984) 667–671.
[21] M.R. Romero, F. Ahumada, F. Garay, Ana Baruzzi, Amperometric biosensor for direct blood lactate detection, Analytical Chemistry 82 (2010) 5568–5572.
[22] F. Garay, C.A. Barbero, Charge neutralization process of mobile species at any distance from the electrode/solution interface. 1. Theory and simulation of concentration and concentration gradients developed during potentiostatic conditions, Analytical Chemistry 78 (2006) 6733–6739.
[23] F. Garay, C.A. Barbero, Charge neutralization process of mobile species developed during potentiodynamic conditions. Part 1: theory, Electroanalytical Chemistry 624 (2008) 218–227.
[24] A. Bergel, M. Comtat, Theoretical evaluation of transient responses of an amperometric enzyme electrode, Analytical Chemistry 56 (1984) 2904–2909.
[25] V. Flexer, K.F.E. Pratt, F. Garay, P.N. Bartlett, E.J. Calvo, Relaxation and Simplex mathematical algorithms applied to the study of steady-state electrochemical responses of immobilized enzyme biosensors: comparison with experiments, Journal of Electroanalytical Chemistry 616 (2008) 87–98.
[26] F. Garay, C.A. Barbero, Charge neutralization process of mobile species at any distance from the electrode/solution interface. 2. Concentration gradients during potential pulse experiments, Analytical Chemistry 78 (2006) 6740–6746.
[27] F. Garay, R.A. Iglesias, C.A. Barbero, Charge neutralization process of mobile species developed during potentiodynamic conditions. Part 2: simulation and fit of probe beam deflection experiments, Journal of Electroanalytical Chemistry 624 (2008) 211–217.
[28] D.J. Leggett, Instrumental simplex optimization: experimental illustrations for an undergraduate laboratory course, Journal of Chemical Education 60 (1983) 707–710.
[29] W.H. Press, S.A. Teukolsky, W.T. Vetterling, B.P. Flannery, Numerical Recipes in Fortran 77: The Art of Scientific Computing, vol. 1, 2nd ed., Cambridge University Press, New York, 1997, pp. 387–406.
[30] M.R. Romero, F. Garay, Ana Baruzzi, Design and optimization of a lactate amperometric biosensor based on lactate oxidase cross-linked with polymeric matrixes, Sensors and Actuators B 131 (2008) 590–595.
[31] M. Powell, J.C. Ball, Y.-C. Tsai, M.F. Suárez, R.G. Compton, Square wave anodic stripping voltammetry at mercury-plated electrodes. Simulation of surface morphology effects on electrochemically reversible, irreversible, and quasi-reversible processes: comparison of thin films and microdroplets, Journal of Physical Chemistry B 104 (2000) 8268–8278.
[32] http://www.millipore.com/catalogue/module/c153#1.
[33] H. Li, R. Luo, Modeling and characterization of glucose-sensitive hydrogel: effect of Young's modulus, Biosensors and Bioelectronics 24 (2009) 3630–3636.
[34] D.R. Lide, CRC Handbook of Chemistry and Physics, 85th ed., CRC Press, FL, USA, 2003, pp. 940–942.
[35] P.A. Sullivan, C.Y. Soon, W.J. Schreurs, J.F. Cutfield, M.G. Shepherd, The structure of L-lactate oxidase from *Mycobacterium smegmatis*, Biochemical Journal 165 (1977) 375–383.
[36] C.P. McMahon, G. Rocchitta, P.A. Serra, S.M. Kirwan, J.P. Lowry, R.D. O'Neill, Control of the oxygen dependence of an implantable polymer/enzyme composite biosensor for glutamate, Analytical Chemistry 78 (2006) 2352–2359.

Biographies

Marcelo Ricardo Romero, Doctor (Universidad Nacional de Córdoba, 2011). Currently he is a postdoctoral researcher at the Department of Organic Chemistry, School of Chemical Science, Universidad Nacional de Córdoba. His fields of interest include electrochemistry, analytical chemistry, polymer science, electronic devices and biosensors.

Ana María Baruzzi, Doctor (Universidad Nacional de Córdoba, 1981). Currently she is a full professor at the Department of Physical Chemistry, School of Chemical Science, Universidad Nacional de Córdoba and Research Fellow of CONICET, Argentina. Her fields of interest include electrochemistry, analytical chemistry, polymer science and biosensors.

Fernando Sebastián Garay, Doctor (Universidad Nacional de Córdoba, 2002). Currently he is an assistant professor at the Department of Physical Chemistry, School of Chemical Science, Universidad Nacional de Córdoba and Research Fellow of CONICET, Argentina. His fields of interest include electrochemistry, numerical and digital simulations, analytical chemistry, in situ techniques, polymer science and biosensors.